https://dx.doi.org/10.1016/j.conbuildmat.2023.131785

Weathering Characteristics of Asphalt Modified by Hybrid of Micro-Nano Tire Rubber and SBS

Xiaoxiao Yu[a], Danning Li[b], Zhen Leng[b], Hongru Yao[c], Shifeng Wang[a, *]

a. School of Chemistry and Chemical Engineering, Shanghai Jiao Tong University, Shanghai 200240, China;

b. Department of Civil and Environmental Engineering, The Hong Kong Polytechnic University, Kowloon, Hong Kong;

c. International Joint Research Center of Green Energy and Chemical Engineering, East China University of Science and Technology, Shanghai 200237, China.

Highlights

- Natural weathering of MNTR/SBS hybrid modified asphalt binder was performed.
- MNTR inhibited oxidation and condensation reaction of asphalt.
- MNTR suppressed the change in molecular weight of asphalt.
- MNTR inhibited physical property deterioration of asphalt during weathering.

Abstract

Tire rubber has been considered as the ideal candidate for improving aging durability of styrene-butadiene-styrene copolymers (SBS) modified asphalt pavement. However, crosslink characteristic of tire rubber affected its dispersion in SBS modified asphalt binder (SMB) and restricted high addition dosage. In this study, microscale and nanoscale tire rubber (MNTR) hybridized SMB with the high dosage was prepared for studying its structural evolution during weathering and physical property variation. Results of gel permeation chromatography and infrared spectroscopy showed that MNTR stabilized the

molecular weight distribution and decreased oxidative condensation reaction of asphalt matrix during weathering, and yet did not prevent the SBS degradation. Structural characteristics revealed that the dissolved rubber and core-shell structured carbon black nanoparticles in MNTR were implanted into the colloid structure of asphalt, inhibiting the weathering reaction including asphalt condensation and asphalt oxidation. Fraass brittleness temperature and modulated differential scanning calorimetry results verified that the hybrid modified asphalt had more stable crack resistance compared with SMB at low temperature, and dynamic shear rheometer experiment proved its stable deformation resistance and excellent elasticity at high temperature during weathering. Accordingly, the addition of high content MNTR strongly improved natural weathering resistance of SMB based on the highly hybridized colloid structure.

Keywords: SBS modified asphalt binder; Micro-nano tire rubber; Natural weathering; Rheology; Chemical structure

1. Introduction

Asphalt pavement is the most common pavement which takes up more than 95 % of the paved highway [1]. The rapidly increasing traffic volume and vehicle load raise demands for the in-service properties, durability, and easy maintenance of pavement. Since modified asphalt binder struggles to satisfy the need of the transportation today, different kinds of modifiers have been applied in the asphalt industry [2], such as styrene-butadiene-styrene (SBS), crumb tire rubber modifier (CRM), etc. Although certain properties of asphalt binder are improved, its aging problem occurs due to natural weathering during the service process [3, 4]. Due to the oxidation reaction of resin and light components,

volatilization of light components and transformation of different components, the composition of asphalt changes with aging, leading to its structural damage [5, 6]. As a consequence, in-service flexible asphalt binder gradually deteriorates into stiff binder, which increases the risk of road damage, especially cracking damage [7-9].

SBS has biphasic structure of cylindrical polystyrene (PS) domains dispersed in a continuous polybutadiene (PB) matrix, endowing asphalt binder with favorable rheological properties [10, 11]. However, allylic hydrogen atoms connected with C=C groups in PB are easy to be attacked by oxygen for its chemical activity. Physical crosslink of PS limits the motion of molecular chains and the self-healing. Thus, biphasic morphology of SBS easily collapses with aging, followed by the unstable rheological properties of SBS modified asphalt binder (SMB) [12-14]. By comparison, the rubberized asphalt binder modified by CRM has been recently reported with superior aging resistance [15-19]. The swelling behavior of CRM particles maintains a relatively stable mechanical condition throughout the aging [20, 21]. However, feasible physical blend of CRM particles and base asphalt builds a heterogeneous system, which has difficulties with high filling content of CRM, restricting further improvement of aging resistance. A relative homogenous terminal blend (rubberized asphalt binder, TB) can be made by increasing the mixing temperature, mixing time and/or shearing rate [22], and its improved aging resistance is owing to the complex composition of CRM and the interaction between asphalt and rubber [6, 23]. However, the components of tire rubber in the TB blend are still unclear due to complicated degradation, aging reaction and interaction of asphalt and rubber during high temperature processing [24].

With the development of devulcanization technology of tire rubber, degraded tire

rubber can be prepared by reactive extrusion [25]. The devulcanization of tire rubber refers to a process during which poly-, di-, mono-sulfidic bonds and even certain carbon-carbon bonds in the main molecular chains are broken [26, 27]. The highly degraded tire rubber in micro-nano size seemed to be compatible with asphalt [28, 29], and could be defined as micro-nano tire rubber (MNTR). The MNTR usage reached up to 25% by weight [30] and endowed the asphalt with outstanding low temperature property and aging resistance [31-33]. MNTR is mainly composed of soluble rubber chain and core-shell structured carbon black nanoparticles, which consists of carbon black covered with tightly and loosely bound rubber in 2 - 15 nm of nanometers [25]. The rubber chains and antioxidants in MNTR are easily exfoliated from the carbon black nanoparticles without the constraints of chemical bonds, and certain rubber molecules are even partially dissolved in the asphalt [29, 30]. Inner active groups in rubber chain and antioxidants acted as radical traps and terminators of the free radical chains through which the photo-oxidative reactions are propagated [16, 18]. Furthermore, high-content carbon black nanoparticles not only stabilized polymer against ultraviolet rays degradation by itself [34], but also showed positive “labyrinth effect”, reducing oxygen diffusion and evaporation of light components [35]. Being benefited from carbon black, exposed active groups and released antioxidants, MNTR could theoretically improve the aging resistance.

Researchers have tried to combine the anti-aging feature of rubberized asphalt and SMB to compensate the insufficient aging resistance of SMB. Previous studies have found that tire rubber was able to improve the aging resistance of SMB in laboratory aging situation by analyzing the change of physical and rheological properties for rubber/SBS hybrid modified asphalt binder [36-39]. Although the aging resistance of degraded tire

rubber modified asphalt with fine dispersion was verified [40, 41], the evolution process of internal multi-scale structure including the oxidation and condensation reaction, molecule-level variation of tire rubber and SBS still remains unclear and the aging mechanism is complex. Furthermore, the methods for accelerated aging in laboratory of asphalt binders often cannot accurately simulate the actual field aging [12, 42], and thereby the effect of MNTR on the aging resistance of SMB under natural weathering needs further research.

For a more comprehensive understanding on the interaction and aging resistance throughout natural weathering, this study aims to investigate the effects of MNTR on asphalt aging or SBS degradation, and the evolution of MNTR by analyzing their structural, rheological, and in-service properties variation. SMB and MNTR/SBS binder were prepared and exposed together with base asphalt to outdoor natural weathering for 12 months. The evolution of chemical structure throughout natural weathering was recorded by infrared spectroscopy (IR), Soxhlet extraction, gel permeation chromatography (GPC) and thermo-gravimetric analysis (TGA) tests. The viscoelastic and in-service properties, including crack resistance and deformation resistance were studied by Fraass brittleness temperature, modulated differential scanning calorimetry tests (MDSC) and dynamical shear rheometer (DSR) tests. The findings are expected to promote theoretical support for the extension of service life of SMB pavement.

2. Experimental

2.1 Materials

Base asphalt was provided by Ssyong Oil Industrial Co., Ltd (Korea) and SBS was

provided by LG Chem. Co., Ltd. (Korea). CRM was supplied by a crumb tire rubber plant of Wuxi (China), and it was prepared into MNTR at 280 °C using a single screw extruder with screw speed of 100 rpm according to Reference [43]. The basic properties of base asphalt, CRM, MNTR and SBS are summarized in Table 1.

Table 1 Basic properties of materials.

Materials	Items	Methods	Units	Results
Base asphalt	Penetration at 25 °C	ASTM D5	0.1 mm	67.2
	Softening point	ASTM D36	°C	47
	Ductility at 10 °C	ASTM D113	cm	92.5
CRM	Source	-	-	Truck tyre
	Diameter	-	mm	0.420–0.425
	Rubber content	-	%	54
	Carbon black content	-		33
	Ash content	-		8
	Additives	-		5
MNTR	Soluble rubber content	Soxhlet extraction	%	71.1
	Mooney viscosity	ASTM D1646	-	15
SBS LG501	S/B	-	-	30/70
	Molecular weight	ASTM D5296	g/mol	120,000

2.2 Preparation of modified asphalt binders

As shown in Figure 2, the preparation of MNTR/SBS binder included two steps. The

MNTR masterbatch (mass ratio of MNTR and base asphalt = 40/60) was firstly prepared by mixing MNTR into asphalt with a high-speed shear (5,000 rpm) for 60 min at 180 °C. Subsequently, the MNTR masterbatch, SBS and base asphalt were mixed together for 40 min at 180 °C with a shearing speed of 4,500 rpm, followed by the addition of sulfur (0.2 wt.%) and a further stirring with a speed of 500 rpm for 180 min at 180 °C. The preparation of SBS modified asphalt binder (SMB) followed the above procedures except for the addition of MNTR. The obtained products were marked as S4 (SBS content of 4 wt.%), C05S4 (MNTR content of 5 wt.% and SBS content of 4 wt.%), C10S4 (MNTR content of 10 wt.% and SBS content of 4 wt.%), C15S4 (MNTR content of 15 wt.% and SBS content of 4 wt.%) and C25S4 (MNTR content of 25 wt.% and SBS content of 4 wt.%), respectively.

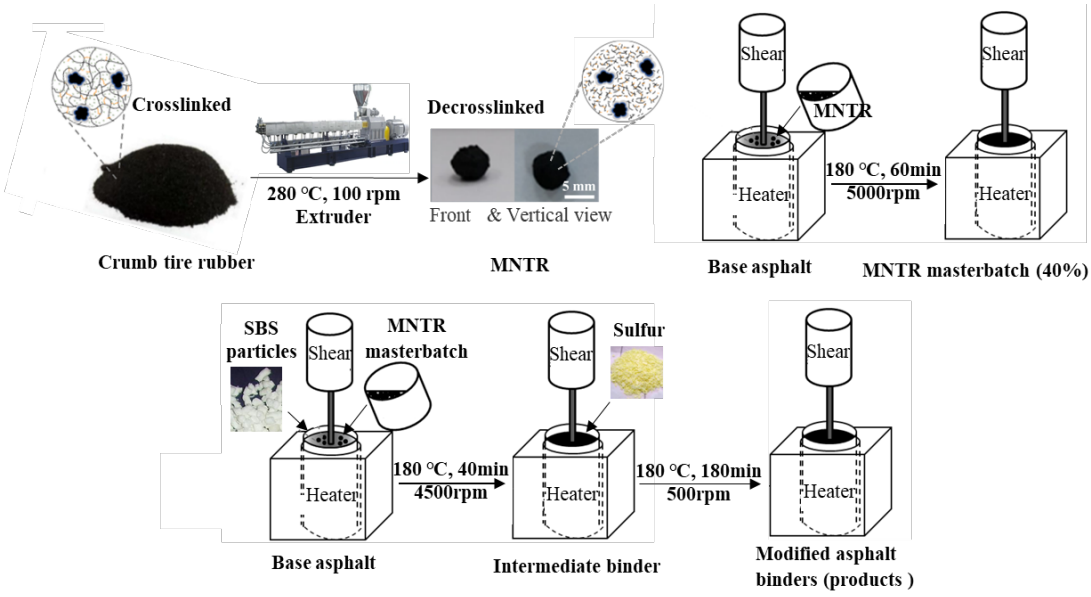

Figure 1 Schematic diagram of the sample preparation.

2.3 Natural weathering of modified asphalt binders

The base asphalt, SMB and C25S4 binder were firstly heated at 150 °C and then

poured into a petri dish with diameter of 10.0 cm. The thickness of 2.0 mm for asphalt sample was selected to capture all weathering information due to that previous literatures reported that the aging effect can propagate for more than 1 mm with the coupling effect of heat and solar radiation [44, 45]. Then, all the samples were placed into an oven (100 °C) to spread flat. Finally, all samples were placed on the rooftop and exposed to natural weathering in Shanghai (31° S, 120° E) with a subtropical monsoon climate from August 2020 to July 2021. The weathering conditions, the geographical location (baike.baidu.com), the typical annual temperature and precipitation situation of Shanghai (tianqi24.com) are shown in Figure 2. The obtained samples were labeled as OBase, OS4, OC25S4, respectively.

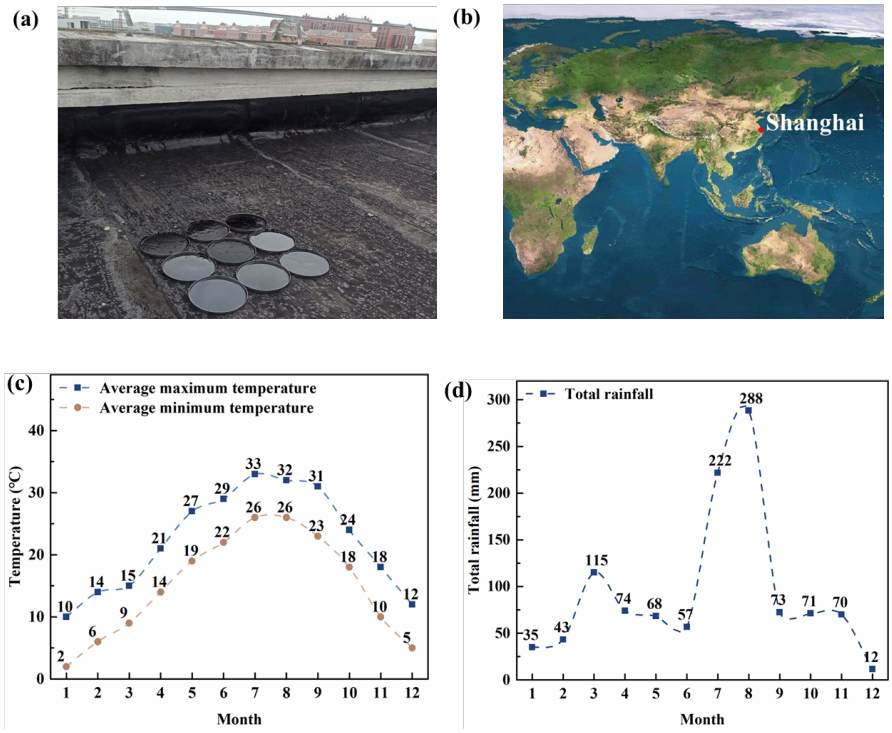

Figure 2 (a) The weathering conditions of asphalts, (b) the geographical location of weathering, (c) and (d) are the typical annual temperature and precipitation situation of

147 Shanghai.

148 *2.4 Structure-property analysis*

149 *2.4.1 Conventional physical properties and optical microscope test*

150 Penetration, ring and ball softening point, ductility, and rotational viscosity of asphalt
151 binders were tested according to ASTM D5, ASTM D36, ASTM D113, and ASTM D 4402,
152 respectively. Fraass brittleness temperature tests of asphalt binders were conducted based
153 on EN 12593. According to EN 12593, a drop of asphalt specimen was placed between
154 heated glass slide and cover, and then pressed into a thin film. An optical microscope (DM
155 4500, Leica, Germany) was employed to observe the morphology of MNTR/SBS binder.

156 *2.4.2 Modulated differential scanning calorimetry (MDSC) test*

157 Glass transition temperature (T_g) of asphalt binder was determined using a differential
158 scanning calorimeter (DSC, TA Q2000, USA) equipped with a refrigerated cooling system
159 (RCS 90). The DSC instrument was calibrated with high-purity sapphire and indium
160 standards. Before actual measurement, the samples were annealed at 150 °C for 2 min to
161 remove the effects of thermal history. The heat flux was modulated on sinusoid between -
162 75 °C and 100 °C at a heating rate of 5 °C/min with a period of 60 s and amplitude of ±
163 2 °C. The DSC cell was purged with dry nitrogen gas at a flow rate of 50 mL/min. Data
164 from the MDSC tests were analyzed with the TA instruments universal analysis 2000
165 software of version 4.5A.

166 *2.4.3 G*, δ, and multiple stress creep and recovery (MSCR) tests*

167 The linear viscoelastic region of each sample was firstly determined by strain sweep

tests so that all the MSCR tests were carried out within the linear viscoelastic region. In order to obtain the curves with G^* and δ values versus temperature at 1 Hz, the frequency sweep tests (0.1 and 30 Hz) were conducted using a dynamical shear rheometer (DSR, TA HR-1, USA) in a wide temperature range from -5 °C to 85 °C with an interval of 10 °C. Parallel plates of 8 mm diameter and 2 mm gap were used for tests between -5 and 25 °C, and 25 mm diameter of parallel plates and 1 mm of gap were used from 35 to 85 °C [46]. The temperature ramp tests were conducted in a temperature range from 40 to 80 °C with a frequency of 10 rad/s and a strain of 0.5%, and relevant fatigue factor ($G^*sin\delta$) at 25 °C was calculated.

The multiple stress creep and recovery (MSCR) tests were performed at 64 °C and 88 °C using 25 mm of parallel plates according to AASHTO T 350. Through preliminary experiment (PG test based on temperature ramp test of original asphalt, 10 rad/s and 0.5% of strain), it was determined that the temperatures ($G^*/sin\delta$ = 1.0 kPa) of base asphalt, S4 and C25S4 were 71 °C, 88 °C and ＞100 °C, respectively. The median value of 88 °C was chosen as the test temperature due to that those three samples had obvious liquidity difference at this temperature. In order to obtain the more comprehensive evaluation and the best of studying rheological characteristic of asphalt, the MSCR tests were also performed at 64 °C. Since there were ten sets of J_{nr} and R for ten creep-relaxation cycles, the average value and error bar of J_{nr} and R were obtained. The strain-time curve of MSCR test was shown in Figure S1, and the J_{nr} and R values of C25S4 tested at 88 °C was shown in Table S1 in supplementary material.

189 *2.4.4 Fourier transform infrared spectroscopy*

190 Structural change of asphalt binders after weathering was studied by an attenuated
191 total reflectance infrared spectrometer (FTIR, Nicolet iz10, USA). Before FTIR tests, all
192 specimens were dried in vacuum at 60 °C for 12 h, and the effect of residual moisture was
193 almost eliminated. The number of scans was 32 and resolution was 4 cm^{-1} between 600 cm^{-1}
194 and 4,000 cm^{-1}. Peak area change for carbonyl (C=O) and sulfoxide (S=O) was used as
195 indicators of oxidation. The carbonyl peak was defined as the band around 1,700 cm^{-1} peak,
196 and the sulfoxide peak was the band around 1,030 cm^{-1}. Aliphatic groups (symmetric and
197 asymmetric bending vibrations around 1,460 and 1,376 cm^{-1}, respectively) were used as
198 reference groups since it was anticipated that these groups were stable throughout
199 weathering [47]. The spectral analysis was carried out using an integration method [48],
200 and the carbonyl index (CI) and sulfoxide index (SI) were calculated using following
201 equations:

202 $$CI = A_{C=O}/A_{\text{ref}} \quad (1)$$

203 $$SI = A_{S=O}/A_{\text{ref}} \quad (2)$$

204 where A_{xx} represents the area of XX peak, C=O ranges from 1,650 cm^{-1} to 1,750 cm^{-1}, S=O
205 ranges from 985 cm^{-1} to 1,070 cm^{-1}, and the reference groups ranges from 1,330 cm^{-1} to
206 1,500 cm^{-1}.

207 *2.4.5 Soluble component fraction test*

208 Soxhlet extraction was conducted for 48 h using toluene as the solvent to separate
209 soluble substance from MNTR/SBS binders. The undissolved rubber was left inside the
210 filter papers, and the soluble substance was dissolved in the flask containing toluene

211 solvent [23]. The soluble substances including asphalt and the soluble rubber were
212 reclaimed by the evaporation method for following GPC tests. The residues (insoluble
213 substances) were dried in vacuum at 60 °C for 6 h till constant weight and collected for
214 TGA tests. The insoluble fraction was calculated by Equation (3).

215 $$g = m_1/m_0 \times 100\% \quad (3)$$

216 where g is insoluble fraction (%), m_0 is initial mass of specimen (g), and m_1 is mass of dried
217 residue (g).

218 *2.4.6 Gel permeation chromatography*

219 Molecular weight distribution of the soluble substances was analyzed by GPC test
220 using a GPC instrument (EcoSEC HLC-8320 GPC, Japan) equipped with a refraction index
221 detector. The soluble substances were dissolved into tetrahydrofuran (THF), and the
222 solutions were then filtered and transferred into the GPC instrument. GPC curve for each
223 specimen was divided into four fractions which were labelled as SMS (small molecular
224 substances, < 10,000 g/mol), LMS (low molecular substances, 10,000 - 40,000 g/mol),
225 MMS (medium molecular substances, 40,000 - 100,000 g/mol) and HMS (high molecular
226 substances, > 100,000 g/mol), respectively [43, 49, 50]. Area normalization method was
227 employed to analyze the GPC results.

228 *2.4.7 Thermo-gravimetric analysis (TGA)*

229 The composition of the insoluble substance was measured by a TGA instrument (TA
230 Q500, USA). The sample of 10 mg was heated from room temperature to 550 °C under
231 nitrogen atmosphere with a heating rate of 20 °C/min, and the atmosphere was then
232 switched to air for further heating to 700 °C.

The experimental process of this study is shown in Figure 3.

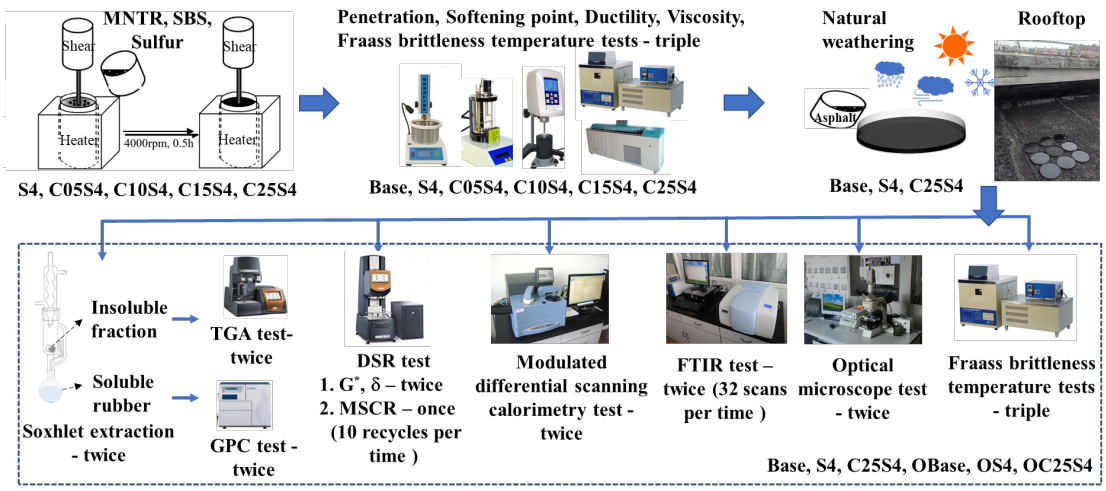

Figure 3 Experimental flow diagram of this study.

3. Results and discussion

3.1 Conventional physical properties

The basic properties of base asphalt and modified asphalts are shown in Table 2 (standard deviation in parentheses). C25S4 had the highest softening point and ductility, the lowest Fraass brittleness temperature and the medium penetration of all asphalts, indicating its superior high- and low- temperature performances. The viscosity of C25S4 at 180 °C was less than 3.0 Pa·s, indicating its processability in engineering. Therefore, C25S4 was selected as representative hybrid modified asphalt for further analysis of aging resistance.

Table 2 Basic properties of base asphalt and modified asphalts.

Items	Penetration at 25 °C / 0.1 mm	Softening point / °C	Ductility at 5 °C / mm	Fraass brittleness temperature / °C	Viscosity at 180 °C / Pa·s
Base	67.2(0.2)	47(0.2)	-	-11.0 (0.4)	-
S4	63.5 (0.2)	80.3 (0.2)	356 (23)	-20.0 (0.4)	-
C05S4	61.7 (0.4)	73.3 (0.3)	342 (9)	-20.0 (0.4)	0.4 (0.02)
C10S4	63.2 (0.3)	80.3 (0.4)	369 (13)	-22.0 (0.6)	0.6 (0.01)
C15S4	67.3 (0.4)	83.7 (0.1)	416 (5)	-23.5 (0.4)	1.0 (0.04)
C25S4	68.9 (0.7)	91.9 (0.1)	432 (9)	-27.5 (0.2)	2.9 (0.09)

3.2 Chemical structure evolution of different asphalt binders

3.2.1 Fourier transform infrared analysis

FTIR spectra of unaged and aged asphalt binders are shown in Figure 4a. The peak intensities at wavenumbers of approximately 1,700 cm^{-1} (C=O) and 1,030 cm^{-1} (S=O) for aged asphalt binders were higher than those of unaged asphalt binders, which indicated the existence of oxidation reaction. Furthermore, the peaks at wavenumbers of approximately 1,100 (attributed to C-O) and 3,400 cm^{-1} (O-H and N-H groups) were observed in spectra of aged asphalt binders, and yet were not observed for unaged asphalt binders, further indicating the oxidation and condensation reactions. These reactions led to an increase in the proportion of polar components and large-size molecules, which further resulted in the decrease of molecular motility and cracks resistance at low temperature [51, 52]. In order to quantitatively study the oxidation reaction degree, CIs and SIs of asphalt binders were calculated and shown in Figure 4b. The lower CI and SI values of OC25S4 compared with OS4 and aged base asphalt demonstrated that the MNTR in modified asphalt had an

inhibition effect on oxidation reaction. The effect might be attributed to the released carbon black particles and soluble rubber in MNTR, which will be further discussed in Section 3.3.

Characteristic peak of butadiene is of importance in evaluating the aging of rubber during weathering [44]. As shown in Figures 4c and 4d, the characteristic peaks of butadiene were observed at 966 cm^{-1} in the spectra of S4, C25S4, OS4, OC25S4. The decreased areas (A_{PB}) of butadiene peaks for aged asphalt binders compared with unaged asphalt binders reflected the degradation of polybutadiene chains in SBS and MNTR during weathering, which also occurred to SMB and MNTR/SBS binder.

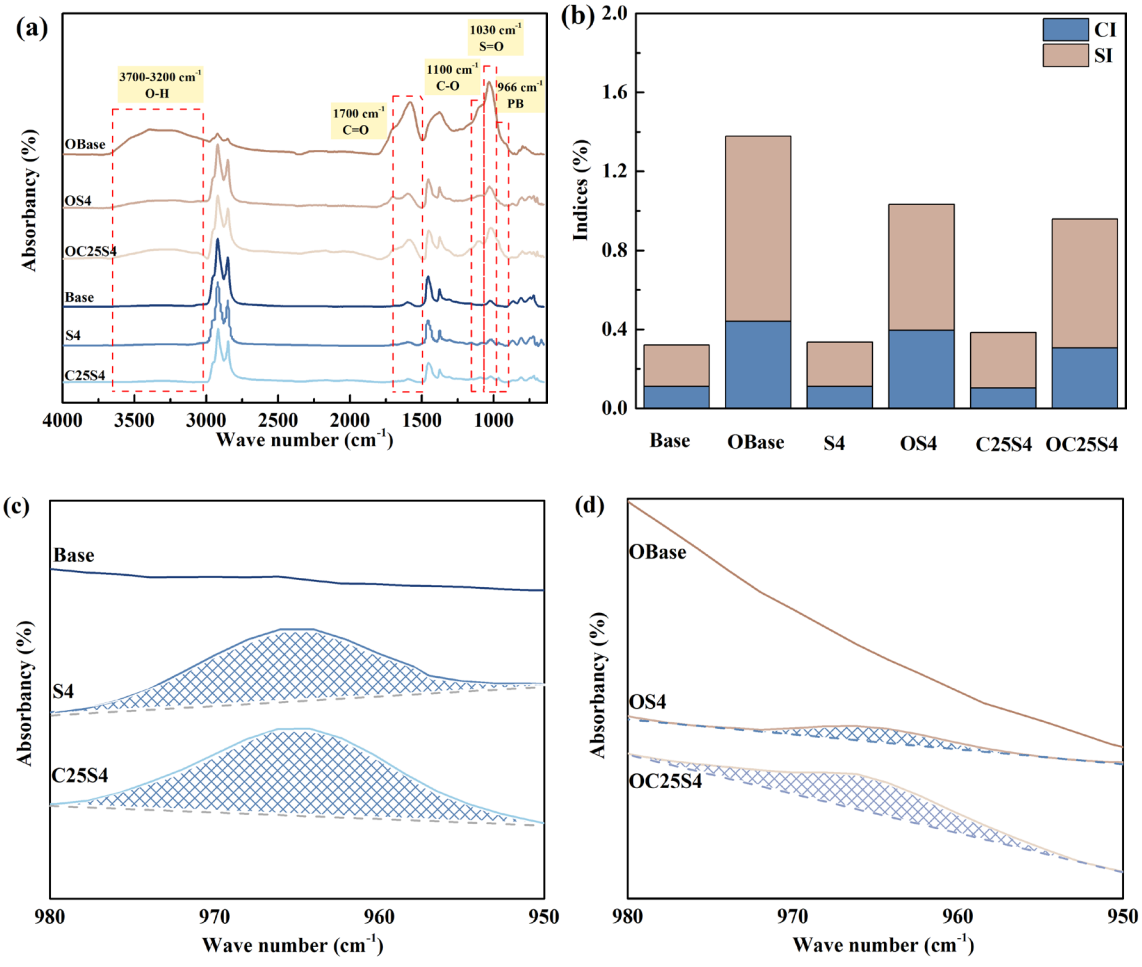

Figure 4 (a) IR spectra, (b) CIs and SIs of Base, OBase, S4, OS4, C25S4, and OC25S4, (c) and (d) are partial IR spectra of unaged and aged asphalt binders, respectively.

3.2.2 Component fraction and molecular weight distribution analysis

The molecular weight distribution curves of soluble substances in unaged and aged asphalt binders for base asphalt, S4, and C25S4 are shown in Figures 5a, 5b, 5c, and 5d, respectively. Base asphalt was mainly composed of small molecular substances (SMS) and low molecular substances (LMS), while S4 and C25S4 consisted of SMS, LMS, medium molecular substances (MMS) and high molecular substances (HMS). The existence of MMS and HMS verified that the addition of SBS and MNTR provided the soluble but large molecular weight polymer (around 10,000 g/mol), which had enormous potential for improving strength of modified asphalt.

As shown in Figure 5a, region area of SMS for aged base asphalt was smaller than that of unaged base asphalt while the opposite tendency set in for LMS region, indicating that natural weathering changed the molecular weight distribution of base asphalt. To be specific, the weight fraction of SMS decreased to 90.3%, and the weight fraction of LMS increased up to 9.7% (in Figure 5e), demonstrating that the fusion and condensation reaction occurred and light components in asphalt volatilized during weathering. For S4, the variation of molecular weight distribution was less obvious compared with base asphalt, but the evolution trend of the molecular weight distribution was similar to base asphalt (Figure 5b), indicated that the fusion and condensation reaction in asphalt dominated the molecular weight variation in SMS and LMS regions. In comparison, the weight fraction

of SMS and LMS for C25S4 had almost no change during weathering (Figures 5c and 5e), and molecular weight distribution for C25S4 during weathering was significantly different from ones observed for base asphalt and S4. These results confirmed the reduced fusion and condensation reaction of maltene, which might be attributed to the microstructure of MNTR/SBS hybrid modified asphalt binder (further discussed in Section 3.3). In addition, the potential degradation of MNTR could decrease the molecular weight and compensate for the increase caused by above chemical reactions of maltene.

In MMS and HMS regions, both the region area and peak position changed during natural weathering for S4 and C25S4 (Figures 5b, 5c and 5e). For S4, the weight fraction of MMS increased during weathering, while the weight fraction of HMS decreased, demonstrating the degradation of SBS. For C25S4, the stabilization effect of MNTR on overall molecular weight distribution of MNTR/SBS binder could be concluded by slight weight fraction change of SMS, LMS, MMS, and HMS regions, which might be responsible for constant physical properties. The high-content polymer in OC25S4 was preserved during weathering, which was beneficial for the high strength of MNTR/SBS binders [53, 54]. Compared with C25S4, HMS fraction of OC25S4 decreased, and insoluble fraction of OC25S4 increased. The degradation of SBS and MNTR could decrease the HMS fraction, and the cross-linking reaction (the transformation of soluble rubbers into insoluble rubber) of MNTR could explain why the insoluble fraction increased. Thus, the SBS degradation, MNTR degradation and their recross-linking reaction were

existing during weathering.

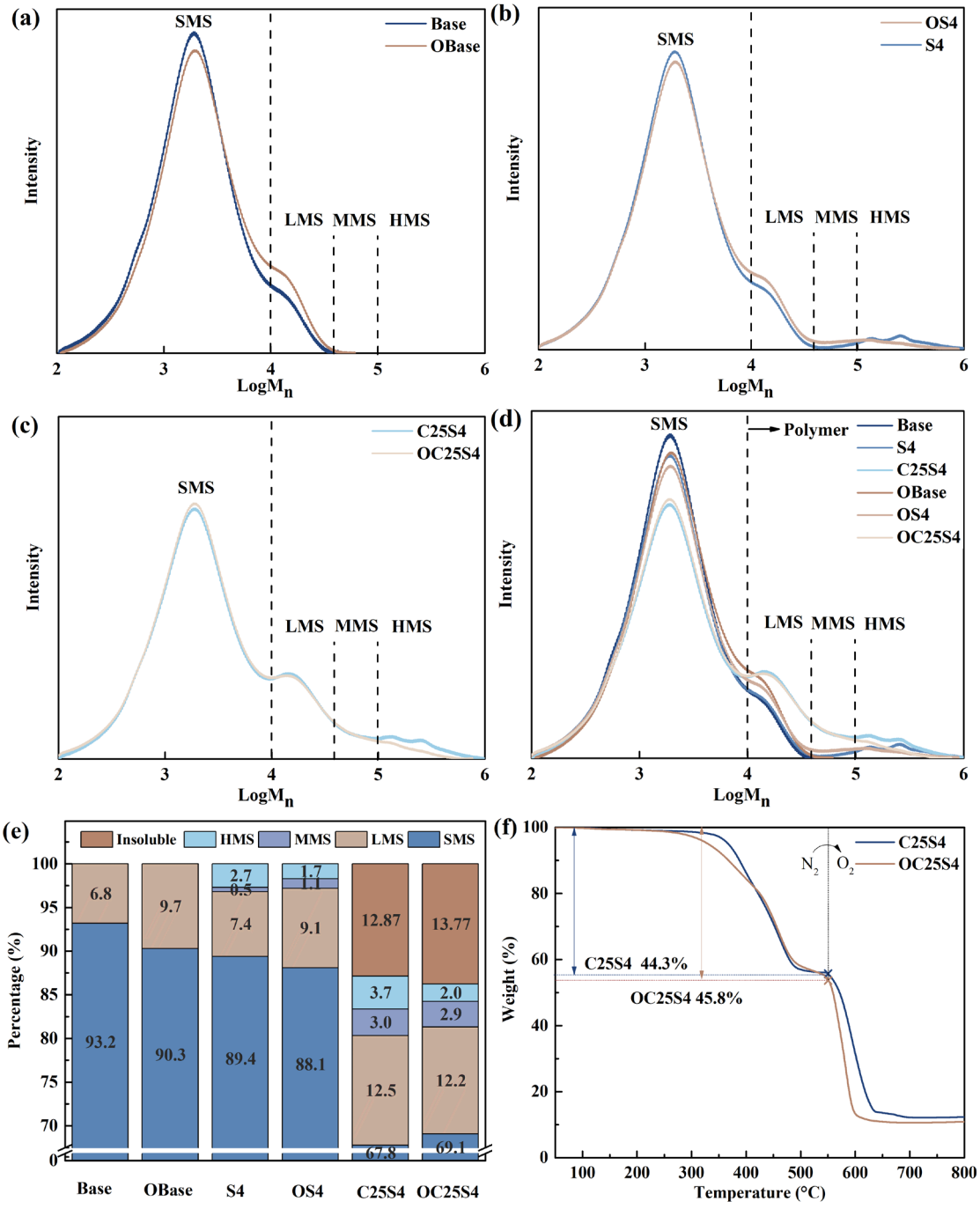

Figure 5 The molecular weight distribution of soluble substances (a) for unaged and aged base asphalt, (b) for S4 and OS4, (c) for C25S4 and OC25S4, (d) unaged and aged

asphalt binders, (e) distribution fractions of SMS, LMS, MMS, and HMS for unaged and aged asphalt binders, and (f) thermal decomposition curves of insoluble substances for C25S4 and OC25S4.

For a more understanding on insoluble substance of C25S4 and OC25S4, the thermal decomposition curves were depicted in Figure 5f. The insoluble substance was composed of carbon black (responding to 550 °C - 800 °C), and bound rubber covered the carbon black. The rubber content in insoluble fraction of OC25S4 (45.8%) was slightly higher than that of C25S4 (44.3%). The increased rubber content in hybrid modified asphalt after weathering further demonstrated the recross-linking reaction. In addition, thermal decomposition reaction of OC25S4 occurred at lower temperature compared with C25S4, indicating the looser structure of OC25S4 due to re-crosslinking rubber of the insoluble substance.

3.3 Morphology of MNTR/SBS hybrid modified asphalt binder

Figures 6a and 6b shows microscopic morphology of unaged and aged MNTR/SBS hybrid modified asphalt binder, and several phases were visible in optical microscope images, indicating the complex aggregation structure of the binder. Carbon black particles with core-shell structure and white SBS phase were randomly distributed in the brown matrix mixed by soluble rubber and asphalt with a colloid structure. After weathering, the morphology of the hybrid asphalt barely changed, indicating its weathering resistance. Figure 6d illustrates microscopic distribution diagram of MNTR/SBS hybrid modified asphalt binder. It could be described that core-shell structured carbon black nanoparticles were implanted into micelle structure and were distributed around the asphaltene, while the

dissolved rubber was mixed with light components consisting of saturates and aromatics.

Since soluble rubber mainly consisted of natural rubber (NR) and synthetic rubber, whose T_g values were remarkably lower than that of asphaltene [55], leading to superior molecule mobility at low temperature. The soluble rubber could also be considered as light components, which endowed the asphaltene micelles with excellent molecule mobility capability. Thus, the crack resistance of MNTR/SBS hybrid modified asphalt binder at low service temperature had potential for being improved.

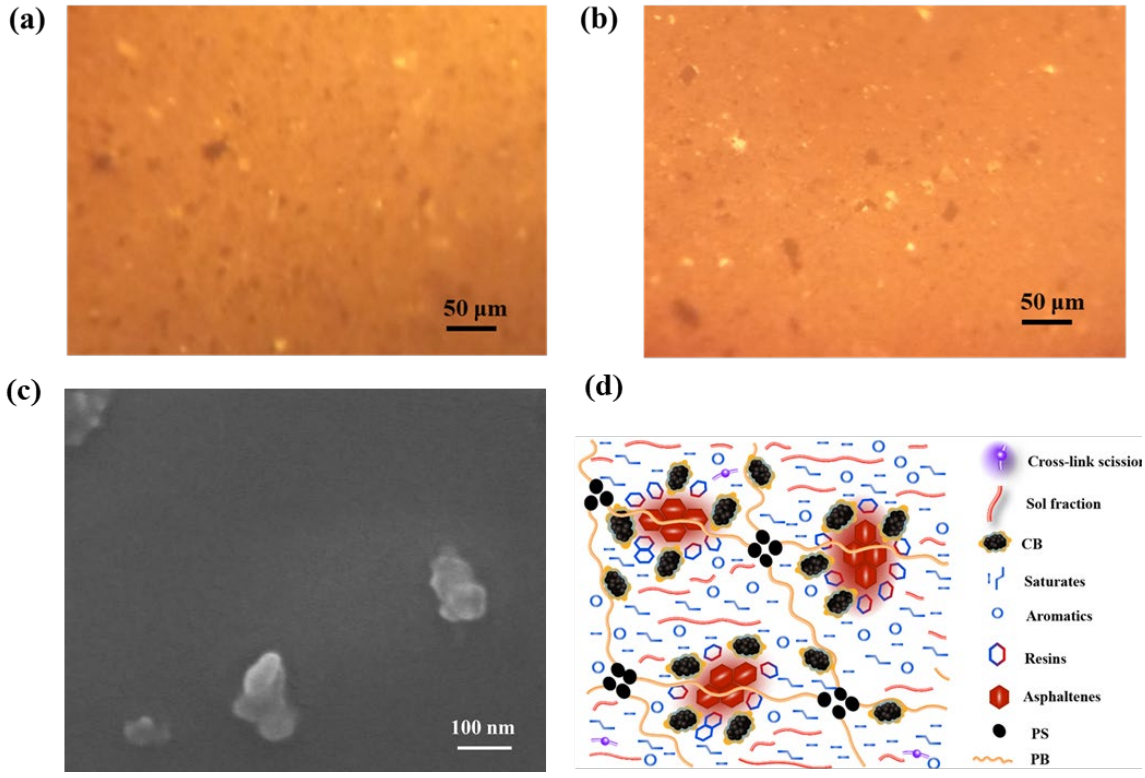

Figure 6 Optical microscope images of (a) unaged and (b) aged MNTR/SBS hybrid modified asphalt binder, (c) SEM image of MNTR and (d) schematic diagram of hybrid asphalt binder.

Figure 6c shows SEM image of MNTR, and core-shell structured carbon black was

observed on nanoscale level. As a common reinforcing agent, carbon black in MNTR strongly contributed to the strength reinforcement of the hybrid asphalt binder again. Besides, soluble rubber with large molecular weight in MNTR could be dissolved in asphalt matrix, which was also helpful to improve strength of modified asphalt [53].

Apart from the shield effect against the ultraviolet rays of the sunlight [17, 35], carbon black particles played a crucial role in maltene phase division. Maltene in base asphalt tended to gather, while it was separated from each other by nanoscale carbon particles in hybrid asphalt binder. This division was of importance for anti-aging property of modified asphalt for it decreased contact area of maltene and its internal reaction. In addition, the dissolved rubber of MNTR improved the viscosity of matrix binder, which affected the oxygen diffusion, leading to aging slowdown of hybrid asphalt binder.

3.4 Physical properties of MNTR/SBS hybrid modified asphalt binder

3.4.1 Rheological behavior

Rheological behavior of asphalt binder was crucial to study the physical properties for it established a direct correlation of structure and in-service properties [49, 51, 56]. Figure 7a shows the variation of G^* with strain at 25 °C for unaged and aged asphalt binders. It was observed that G^* of all asphalt binders barely changed between 0.1% and 2% when a small oscillation strain of 0.5% was obtained, belonging in linear viscoelastic region. The variations of G^* and phase angles with temperature of unaged asphalt binders are illustrated in Figure 7b. In high temperature range of 40 - 80 °C, the higher G^* and lower phase angles of unaged and aged C25S4 compared with base asphalt and S4 demonstrated the improved strength, which verified the extrapolation that MNTR improved the strength of asphalt in

374 GPC analysis. In addition, the G^* of C25S4 was higher than that of asphalt binder modified
375 with reported tire rubber modified asphalt [17], indicating the better high-temperature
376 performance of C25S4. In the low temperature range of -20 - 0 °C, unaged and aged C25S4
377 showed the lower G^* and higher phase angles compared with base asphalt and S4,
378 demonstrating the higher flexibility of hybrid modified asphalt binder. This indicated that
379 the addition of MNTR improved the crack resistance, which might be related to the
380 improved segment mobility or molecule mobility.

381 As shown in Figures 7c and 7d, compared with base asphalt and S4 in the low
382 temperature range, the remarkable change of G^* and δ of aged base asphalt and OS4
383 verified the asphalt hardening. However, the rheological parameters of C25S4 almost had
384 no change (Figure 7e), which indicated the shielding effect of MNTR on weathering of the
385 binder. The shielding mechanism was supposed to be related to the inhibited oxidation
386 reaction and condensation reaction through IR and GPC analysis. Furthermore, fatigue
387 factor of asphalt binders was calculated and shown in Figure 7f. The fatigue factor of
388 C25S4 was lower than that of S4 and base asphalt. During natural weathering, the variation
389 of fatigue factor for C25S4 was remarkably smaller than those of base asphalt and S4, and
390 this variation tendency was similar to the variation of G^* and phase angle. These results
391 indicated the higher fatigue resistance and weathering resistance of C25S4.

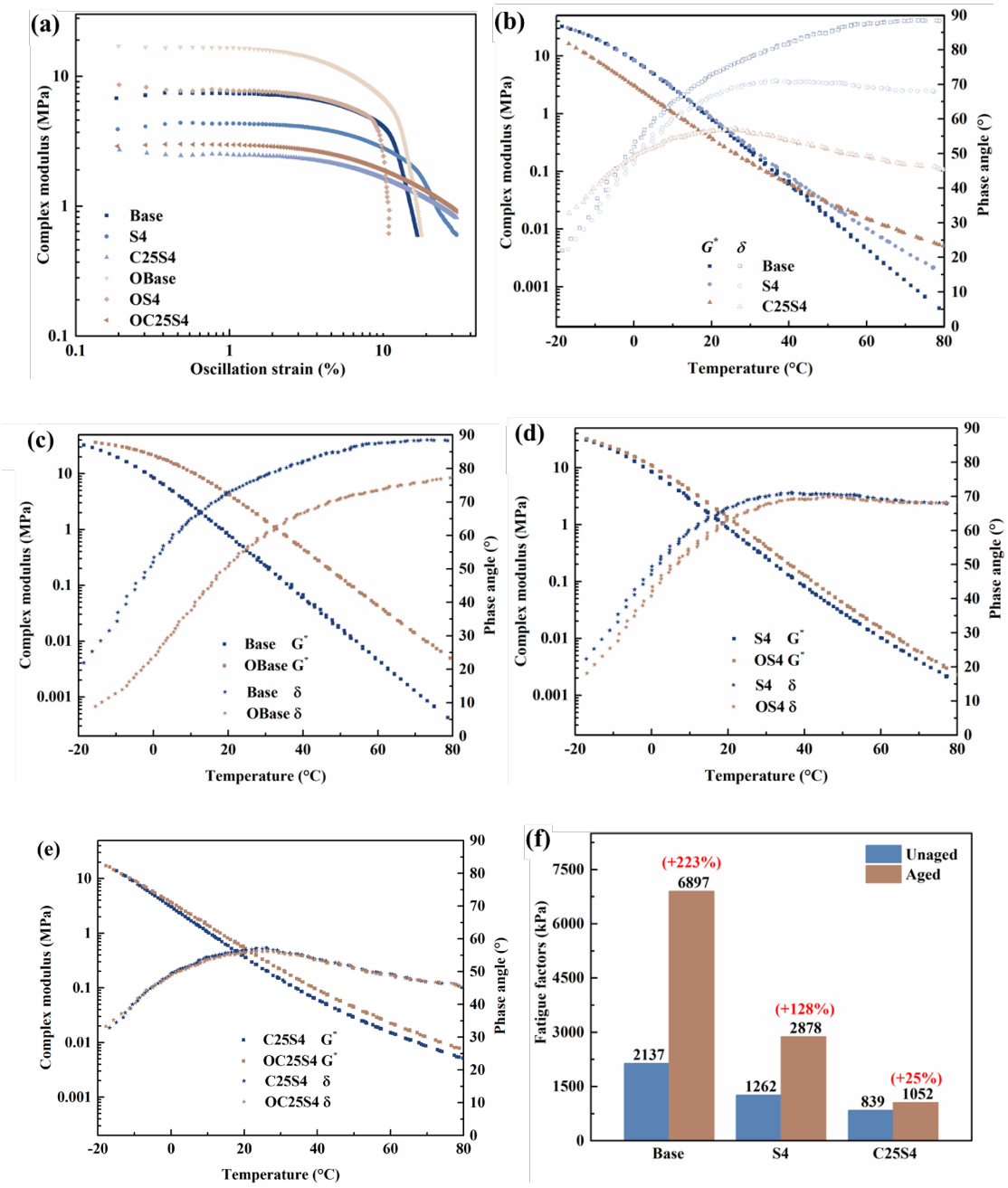

Figure 7 (a) Complex modulus with strain at 25 °C for unaged and aged asphalt binders. (b) Complex modulus and phase angles with temperature at 1 Hz for unaged asphalt binders, (c) for unaged and aged base asphalt binder, (d) for S4 and OS4 and (e) for C25S4 and OC25S4. (f) The fatigue factor of unaged and aged asphalt binders (25 °C).

3.4.2 Deformation resistance at high service temperature

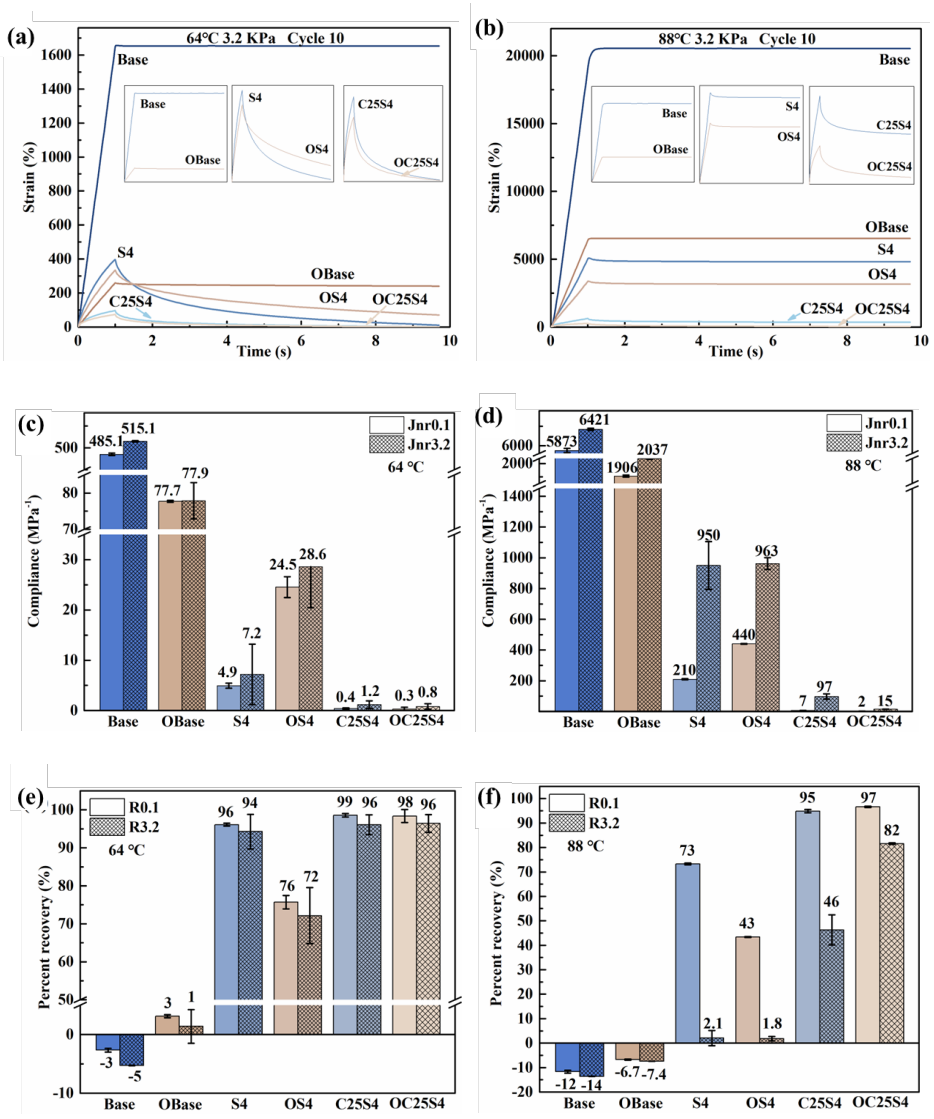

Figure 8 Strain response curves (the tenth cycle of MSCR tests) measured at (a) 64 °C and (b) 88 °C; average compliance (J_{nr}) measured at (c) 64 °C and (d) 88 °C; average percent recovery (R) measured at (e) 64 °C and (f) 88 °C.

Although the G^* value at high temperature reflected rutting resistance of asphalt, it was measured within the linear viscoelastic (LVE) region [57]. To further study actual deformation resistance, the MSCR tests in the nonlinear range were conducted at 64 °C

and 88 °C, which was in correlation with field rutting for allowing for the viscous flow and elasticity of materials. As shown in Figures 8a and 8b, the strains of both C25S4 and OC25S4 were remarkably lower than those of other asphalt binders, and both C25S4 and OC25S4 had considerable recoverable deformations, indicating the higher rutting resistance of hybrid modified asphalt. This was also verified by the lower J_{nr} value (Figures 8c and 8d) and the higher R value (Figures 8e and 8f) compared with base asphalt and S4. These results provided clear evidences for the good and stable deformation resistance and elasticity of MNTR/SBS binder during natural weathering, which verified the conclusion in GPC and rheological analysis.

The J_{nr} tested at 64 °C and 0.1 kPa of unaged base asphalt (485 MPa^{-1}) was six times higher than that of aged base asphalt (78 MPa^{-1}), and the J_{nr} tested at 64 °C and 0.1 kPa of OS4 (25 MPa^{-1}) was nearly five times higher than that of S4 (5 MPa^{-1}). However, the J_{nr} value of OC25S4 (0.3 MPa^{-1}) was close to that of C25S4 (0.4 MPa^{-1}). The change range of J_{nr} for C25S4 was smaller than that of S4 or base asphalt, and the similar phenomenon can be found in the J_{nr} and R values tested in other experimental conditions, indicating the introduction of MNTR inhibited the rheological evolution.

3.4.3 Crack resistance at low service temperature

Top-down cracks in the asphalt pavement is always caused by the increased stiffness of the binder under natural weathering. Fraass brittleness temperature test can be used to characterize the crack resistance of asphalt binder at low service temperature. As shown in Figure 9a, the Fraass brittleness temperatures of MNTR/SBS binders were lower than those of base asphalt and SMB, and were also lower than those of CRM particles modified asphalt binders reported in literatures [58]. The reduced Fraass brittleness temperature

suggested that MNTR enhanced the crack resistance, which could be related to the flexibility improvement of segments or molecules. The flexibility was able to be characterized by MDSC tests [59] and was indirectly quantified by the glass transition temperature (T_g). As shown in Figure 9b, the T_g of MNTR/SBS binder was remarkably lower than those of SMB and base asphalt, indicating its improved molecule mobility. The improvement might be attributed to the addition of flexibility segments, which was confirmed by the existence of the peak around -36.9 °C in the low temperature range.

Compared with unaged asphalt binders, the higher Fraass brittleness temperatures of all aged asphalt binders indicated that natural weathering remarkably hardened the asphalt [60]. The retention ratio of Fraass brittleness temperatures after weathering for MNTR/SBS binders was in the range of 71-82%, which was remarkably higher than those of base asphalt (45%) and SMB (60%). This result demonstrated that the introduction of MNTR inhibited the deterioration of cracks resistance for MNTR/SBS binder throughout weathering, agreeing with the rheological analysis in Section 3.4.1. The inhibited oxidation reactions verified by IR results could well explain the shielding mechanism of crack resistance for hybrid modified asphalt binder.

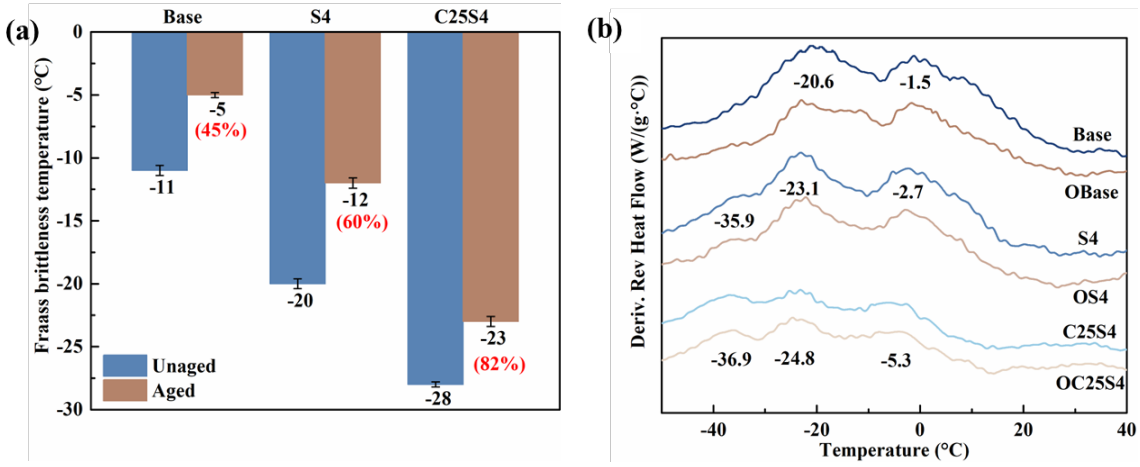

Figure 9 (a) Fraass brittleness temperatures and (b) derivative of reversible heat flow curves of unaged and aged asphalt binders.

4. Conclusion

The natural weathering characteristics of hybrid modified asphalt through adding high-content MNTR into SBS modified asphalt (SMB) was investigated by analyzing its microstructure and physical properties. The main findings were concluded as follows:

- MNTR inhibited the oxidation reaction, fusion and condensation reaction of asphalt, which was demonstrated by the decreased oxidation index, stable molecular distribution, and slightly changed properties of MNTR/SBS hybrid modified asphalt binder.
- MNTR alleviated the deterioration of molecular weight distribution for the hybrid asphalt binders.
- Slight recross-linking or degradation reactions occurred to MNTR/SBS binder during natural weathering.
- The variation of rheological parameters, Fraass brittleness temperature of aged hybrid modified asphalt binder were remarkably lower than those of base asphalt and SMB, indicating its high weathering resistance.

This study verified that MNTR improved the natural weathering resistance of asphalt binder by inhibiting chemical reactions and alleviating the change of molecular weight distribution. Accordingly, addition of MNTR into SMB was a feasible method to improve the in-service performance of asphalt pavement, and yet its practice and microanalysis of MNTR/SBS binders deserved further investigation in future.

Acknowledgements

The authors are grateful for the foundation supported by Ministry of Science and Technology (2021YFE0105200) and National Centre for Research and Development (WPC 2/SUSDEV4REC/2021). (Financial support)

References

[1] T. Xu, X. Huang, Investigation into causes of in-place rutting in asphalt pavement, Construction and Building Materials, 28 (2012), 525-530, https://doi.org/10.1016/j.conbuildmat.2011.09.007.

[2] J. Zhu, B. Birgisson, N. Kringos, Polymer modification of bitumen: Advances and challenges, European Polymer Journal, 54 (2014), 18-38, https://doi.org/10.1016/j.eurpolymj.2014.02.005.

[3] Y. Zhang, Z. Leng, Quantification of bituminous mortar ageing and its application in ravelling evaluation of porous asphalt wearing courses, Materials & Design, 119 (2017), 1-11, https://doi.org/10.1016/j.matdes.2017.01.052.

[4] A. Behnood, M. Modiri Gharehveran, Morphology, rheology, and physical properties of polymer-modified asphalt binders, European Polymer Journal, 112 (2019), 766-791, https://doi.org/10.1016/j.eurpolymj.2018.10.049.

[5] H. Soenen, X. Carbonneau, X. Lu, C. Robertus, B. Tapin, Rheological and chemical properties of field aged binders and their variation within the wearing course, Road Materials and Pavement Design, (2021), 1-19, https://doi.org/10.1080/14680629.2021.1994450.

[6] H. Wang, X. Liu, P. Apostolidis, M. van de Ven, S. Erkens, A. Skarpas, Effect of laboratory aging on chemistry and rheology of crumb rubber modified bitumen, Materials and Structures, 53 (2020), 26-40, https://doi.org/10.1617/s11527-020-1451-9.

[7] S. Zhang, Y. Cui, W. Wei, Low-temperature characteristics and microstructure of asphalt under complex aging conditions, Construction and Building Materials, 303 (2021), 124408, https://doi.org/10.1016/j.conbuildmat.2021.124408.

[8] R. Rahbar-Rastegar, J.S. Daniel, E.V. Dave, Evaluation of viscoelastic and fracture properties of asphalt mixtures with long-term laboratory conditioning, Transportation Research Record, 2672 (2018), 503-513, https://doi.org/10.1177/0361198118795012.

[9] Y. Ruan, R.R. Davison, C.J. Glover, Oxidation and viscosity hardening of polymer-modified asphalts, Energy & Fuels, 17 (2003), 991-998, http://doi.org/10.1021/ef0202211.

[10] A. Schaur, S. Unterberger, R. Lackner, Impact of molecular structure of SBS on thermomechanical properties of polymer modified bitumen, European Polymer Journal, 96 (2017), 256-265, https://doi.org/10.1016/j.eurpolymj.2017.09.017.

[11] M.d.C.C. Lucena, S.d.A. Soares, J.B. Soares, Characterization and thermal behavior of polymer-modified asphalt, Materials Research, 7 (2004), 529-534,

https://doi.org/10.1590/s1516-14392004000400004
[12] X. Zhao, Rheological and structural evolution of SBS modified asphalts under natural weathering, Fuel, 184 (2016), 242-247, https://doi.org/10.1016/j.fuel.2016.07.018.
[13] M.S. Cortizo, D.O. Larsen, H. Bianchetto, J.L. Alessandrini, Effect of the thermal degradation of SBS copolymers during the ageing of modified asphalts, Polymer Degradation and Stability, 86 (2004), 275-282, https://doi.org/10.1016/j.polymdegradstab.2004.05.006.
[14] R. tur Rasool, Y. Hongru, A. Hassan, S. Wang, H. Zhang, In-field aging process of high content SBS modified asphalt in porous pavement, Polymer degradation and stability, 155 (2018), 220-229, https://doi.org/10.1016/j.polymdegradstab.2018.07.023.
[15] I.L. Howard, G.L. Baumgardner, W.S. Jordan, J.M. Hemsley, C. Hopkins, Comparing Ground Tire Rubber, Styrene-Butadiene-Styrene, and GTR-SBS Hybrids as Asphalt Binder Modifiers, Journal of Materials in Civil Engineering, 33 (2021), 04021091, http://doi.org/10.1061/(ASCE)MT.1943-5533.0003709.
[16] J. Geng, M. Chen, C. Xia, X. Liao, Z. Chen, H. Chen, Y. Niu, Quantitative determination for effective rubber content in aged modified asphalt binder, Journal of Cleaner Production, 331 (2022), 129978, https://doi.org/10.1016/j.jclepro.2021.129978.
[17] Q. Wang, S. Li, X. Wu, S. Wang, C. Ouyang, Weather aging resistance of different rubber modified asphalts, Construction and Building Materials, 106 (2016), 443-448, https://doi.org/10.1016/j.conbuildmat.2015.12.138.
[18] S. Wang, Q. Wang, S. Li, Thermooxidative aging mechanism of crumb-rubber-modified asphalt, Journal of Applied Polymer Science, 133 (2016), 43323, https://doi.org/10.1002/app.43323.
[19] M. Jamal, M. Lanotte, F. Giustozzi, Exposure of crumb rubber modified bitumen to UV radiation: A waste-based sunscreen for roads, Journal of Cleaner Production, 348 (2022), 131372, https://doi.org/10.1016/j.jclepro.2022.131372.
[20] H. Wang, X. Liu, P. Apostolidis, S. Erkens, A. Skarpas, Experimental investigation of rubber swelling in bitumen, Transportation Research Record, 2674 (2020), 203-212, https://doi.org/10.1177/0361198120906423.
[21] D. Li, Z. Leng, F. Zou, H. Yu, Effects of rubber absorption on the aging resistance of hot and warm asphalt rubber binders prepared with waste tire rubber, Journal of Cleaner Production, 303 (2021), 127082, https://doi.org/10.1016/j.jclepro.2021.127082.
[22] T.C. Billiter, J.S. Chun, R.R. Davison, C.J. Glover, J.A. Bullin, Investigation of the curing variables of asphalt-rubber binder, Petroleum Science and Technology, 15 (1997), 445-469, https://doi.org/10.1080/10916469708949669.
[23] D. Li, Z. Leng, H. Wang, R. Chen, F. Wellner, Structural and mechanical evolution of the multiphase asphalt rubber during aging based on micromechanical back-calculation and experimental methods, Materials & Design, 215 (2022), 110421, https://doi.org/10.1016/j.matdes.2022.110421.
[24] S. Wang, W. Huang, P. Lin, Z. Wu, C. Kou, B. Wu, Chemical, physical, and rheological evaluation of aging behaviors of terminal blend rubberized asphalt binder, Journal of Materials in Civil Engineering, 33 (2021), 04021302, http://doi.org/10.1061/(ASCE)MT.1943-5533.0003931.
[25] S. Li, C. Wan, S. Wang, Z. Yong, Separation of core-shell structured carbon black nanoparticles from waste tires by light pyrolysis, Composites Science & Technology, 135

(2016), 13-20, https://doi.org/10.1016/j.compscitech.2016.09.009.
[26] M. Myhre, D.A. MacKillop, Rubber Recycling, Rubber Chemistry and Technology, 75 (2002), 429-474, http://doi.org/10.5254/1.3547678.
[27] S. Wang, D. Cheng, F. Xiao, Recent developments in the application of chemical approaches to rubberized asphalt, Construction & Building Materials, 131 (2017), 101-113, https://doi.org/10.1016/j.conbuildmat.2016.11.077.
[28] R.T. Rasool, S. Pan, S. Wang, Thermal analysis on the interactions among asphalt modified with SBS and different degraded tire rubber, Construction & Building Materials, 182 (2018), 134-143, https://doi.org/10.1016/j.conbuildmat.2018.06.104.
[29] P. Song, X. Zhao, X. Cheng, S. Li, S. Wang, Recycling the nanostructured carbon from waste tires, Composites Communications, 7 (2018), 12-15, https://doi.org/10.1016/j.coco.2017.12.001.
[30] X. Wu, S. Wang, R. Dong, Lightly pyrolyzed tire rubber used as potential asphalt alternative, Construction and Building Materials, 112 (2016), 623-628, https://doi.org/10.1016/j.conbuildmat.2016.02.208.
[31] K.-D. Jeong, S.-J. Lee, S.N. Amirkhanian, K.W. Kim, Interaction effects of crumb rubber modified asphalt binders, Construction and Building Materials, 24 (2010), 824-831, https://doi.org/10.1016/j.conbuildmat.2009.10.024.
[32] F.J. Navarro, P. Partal, F. Martínez-Boza, C. Gallegos, Influence of Crumb Rubber Concentration on the Rheological Behavior of a Crumb Rubber Modified Bitumen, Energy & Fuels, 19 (2005), 1984-1990, https://doi.org/10.1021/ef049699a.
[33] A.F. de Almeida Júnior, R.A. Battistelle, B.S. Bezerra, R. de Castro, Use of scrap tire rubber in place of SBS in modified asphalt as an environmentally correct alternative for Brazil, Journal of Cleaner Production, 33 (2012), 236-238, https://doi.org/10.1016/j.jclepro.2012.03.039.
[34] M. Liu, A.R. Horrocks, Effect of Carbon Black on UV stability of LLDPE films under artificial weathering conditions, Polymer Degradation and Stability, 75 (2002), 485-499, https://doi.org/10.1016/S0141-3910(01)00252-X.
[35] S. Filippi, M. Cappello, M. Merce, G. Polacco, Effect of Nanoadditives on Bitumen Aging Resistance: A Critical Review, Journal of Nanomaterials, 2018 (2018), 2469307, http://doi.org/10.1155/2018/2469307.
[36] R. Wang, G. Xu, X. Chen, W. Zhou, H. Zhang, Evaluation of aging resistance for high-performance crumb tire rubber compound modified asphalt, Construction and Building Materials, 218 (2019), 497-505, https://doi.org/10.1016/j.conbuildmat.2019.05.124.
[37] S. Wang, W. Huang, Investigation of aging behavior of terminal blend rubberized asphalt with SBS polymer, Construction and Building Materials, 267 (2021), 120870, https://doi.org/10.1016/j.conbuildmat.2020.120870.
[38] Q. Fu, G. Xu, X. Chen, J. Zhou, F. Sun, Rheological properties of SBS/CR-C composite modified asphalt binders in different aging conditions, Construction and Building Materials, 215 (2019), 1-8, https://doi.org/10.1016/j.conbuildmat.2019.04.076.
[39] L. Xiang, J. Cheng, S. Kang, Thermal oxidative aging mechanism of crumb rubber/SBS composite modified asphalt, Construction and Building Materials, 75 (2015), 169-175, https://doi.org/10.1016/j.conbuildmat.2014.08.035.
[40] R. tur Rasool, S. Wang, Y. Zhang, Y. Li, G. Zhang, Improving the aging resistance

of SBS modified asphalt with the addition of highly reclaimed rubber, Construction and Building Materials, 145 (2017), 126-134, https://doi.org/10.1016/j.conbuildmat.2017.03.242.

[41] G. Xu, Y. Yu, J. Yang, T. Wang, P. Kong, X. Chen, Rheological and aging properties of composite modified bitumen by styrene–butadiene–styrene and desulfurized crumb rubber, Polymers, 13 (2021), 3037-3054, https://doi.org/10.3390/polym13183037.

[42] J. Crucho, L. Picado-Santos, J. Neves, S. Capitão, I.L. Al-Qadi, Tecnico accelerated ageing (TEAGE) – a new laboratory approach for bituminous mixture ageing simulation, International Journal of Pavement Engineering, 21 (2020), 753-765, http://doi.org/10.1080/10298436.2018.1508845.

[43] X. Yu, W. Yang, L. Zhang, K. Formela, S. Wang, Impact and stretching standardized tests as useful tools for assessment of viscoelastic behavior for highly rubberized asphalt binder, Construction and Building Materials, 348 (2022), 128650, https://doi.org/10.1016/j.conbuildmat.2022.128650.

[44] M. Hu, J. Ma, D. Sun, S. Ling, T. Lu, H. Ni, Understanding the Aging Depth Gradient Distribution of High Viscosity Modified Asphalt under the Effect of Solar Radiation and Diffuse Oxygen, ACS Sustainable Chemistry & Engineering, 9 (2021), 15175-15189, https://doi.org/10.1021/acssuschemeng.1c04395.

[45] W.D. Fernández-Gómez, H. Rondón Quintana, F. Reyes Lizcano, A review of asphalt and asphalt mixture aging: Una revisión, Ingeniería e Investigación, 33 (2013), 5-12,

[46] G.D. Airey, Rheological evaluation of ethylene vinyl acetate polymer modified bitumens, Construction and Building Materials, 16 (2002), 473-487, https://doi.org/10.1016/S0950-0618(02)00103-4.

[47] J. Lamontagne, P. Dumas, V. Mouillet, J. Kister, Comparison by Fourier transform infrared (FTIR) spectroscopy of different ageing techniques: application to road bitumens, Fuel, 80 (2001), 483-488, https://doi.org/10.1016/S0016-2361(00)00121-6.

[48] B. Hofko, L. Porot, A. Falchetto Cannone, L. Poulikakos, L. Huber, X. Lu, K. Mollenhauer, H. Grothe, FTIR spectral analysis of bituminous binders: reproducibility and impact of ageing temperature, Materials and Structures, 51 (2018), 45-60, https://doi.org/10.1617/s11527-018-1170-7.

[49] M. Cappello, S. Filippi, Y. Hung, M. Losa, G. Polacco, Apparent Molecular Weight Distributions for Investigating Aging in Polymer-Modified Bitumen, Advances in Polymer Technology, 2021 (2021), 3660646, http://doi.org/10.1155/2021/3660646.

[50] P. Lin, W. Huang, Y. Li, N. Tang, F. Xiao, Investigation of influence factors on low temperature properties of SBS modified asphalt, Construction and Building Materials, 154 (2017), 609-622, https://doi.org/10.1016/j.conbuildmat.2017.06.118.

[51] Y. Wang, W. Wang, L. Wang, Understanding the relationships between rheology and chemistry of asphalt binders: A review, Construction and Building Materials, 329 (2022), 127161, https://doi.org/10.1016/j.conbuildmat.2022.127161.

[52] R. Maharaj, A comparison of the composition and rheology of Trinidad lake asphalt and Trinidad petroleum bitumen, International Journal of Applied Chemistry, 5 (2009), 169+, https://www.researchgate.net/publication/289017637.

[53] R.W. Nunes, J.R. Martin, J.F. Johnson, Influence of molecular weight and molecular weight distribution on mechanical properties of polymers, Polymer Engineering

& Science, 22 (1982), 205-228, https://doi.org/10.1002/pen.760220402.
[54] J.L. Leblanc, Rubber–filler interactions and rheological properties in filled compounds, Progress in Polymer Science, 27 (2002), 627-687, https://doi.org/10.1016/S0079-6700(01)00040-5.
[55] P. Kriz, Glass transition and physical hardening of asphalts, University of Calgary, Calgary, 2009, http://dx.doi.org/10.11575/PRISM/2605.
[56] J. Dealy, R. Larson, Linear viscoelasticity-behavior of molten polymers, in: J. Dealy, R. Larson (Eds.) Structure and Rheology of Molten Polymers: From Structure to Flow Behavior and Back Again, Hanser Publisher, Munich, 2006, 1-61, http://doi.org/10.3139/9783446412811.005.
[57] H. Liu, W. Zeiada, G.G. Al-Khateeb, A. Shanableh, M. Samarai, Use of the multiple stress creep recovery (MSCR) test to characterize the rutting potential of asphalt binders: A literature review, Construction and Building Materials, 269 (2021), 121320, https://doi.org/10.1016/j.conbuildmat.2020.121320.
[58] T. Wang, F. Xiao, S. Amirkhanian, W. Huang, M. Zheng, A review on low temperature performances of rubberized asphalt materials, Construction and Building Materials, 145 (2017), 483-505, https://doi.org/10.1016/j.conbuildmat.2017.04.031.
[59] G.M. Memon, B.H. Chollar, Glass transition measurements of asphalts by DSC, Journal of thermal analysis, 49 (1997), 601-607, http://doi.org/10.1007/BF01996742.
[60] A.K. Ghosh, P. Chaudhuri, B. Kumar, S.S. Panja, Review on aggregation of asphaltene vis-a-vis spectroscopic studies, Fuel, 185 (2016), 541-554, https://doi.org/10.1016/j.fuel.2016.08.031.